McGill/93-9
TPI-MINN-93/18-T
May 1993

Dilepton Production in Nucleon-Nucleon Reactions With and Without Hadronic Inelasticities

Kevin Haglin[a,d] and Charles Gale[b,c]

Theoretical Physics Institute, University of Minnesota
Minneapolis, MN 55455

and

Physics Department, McGill University, 3600 University Street
Montréal, QC, Canada H3A 2T8

Abstract

We calculate elementary proton-proton and neutron-proton bremsstrahlung and their contribution to the e^+e^- invariant mass distribution. At 4.9 GeV, the proton-proton contribution is larger than neutron-proton, but it is small compared to recent data. We then make a first calculation of bremsstrahlung in nucleon-nucleon reactions with multi-hadron final states. Again at 4.9 GeV, the many-body bremsstrahlung is larger than simple nucleon-nucleon bremsstrahlung by more than an order of magnitude in the low-mass region. When the bremsstrahlung contributions are summed with Dalitz decay of the η, radiative decay of the Δ and from two-pion annihilation, the result matches recent high statistics proton-proton data from the Dilepton Spectrometer collaboration.

[a]internet: haglin@hep.physics.mcgill.ca.
[b]internet: gale@hep.physics.mcgill.ca
[c]Permanent address: Physics Department, McGill University, 3600 University Street, Montréal QC, Canada H3A 2T8
[d]Present address: Physics Department, McGill University, 3600 University Street, Montréal QC, Canada H3A 2T8; After 1 September 1993: Michigan State University, East Lansing, Michigan 48824

1 Introduction

Electromagnetic probes are very well suited for studies of strongly interacting particles under conditions ranging from free space to nuclear matter at high energies and densities. They carry away virtually unaltered information about the reaction since they do not suffer strong-interaction rescattering. Our understanding of their properties continues to improve with the aid of both theoretical and experimental efforts. For instance, recent high statistics experiments have been carried out at Lawrence Berkeley Laboratory by the Dilepton Spectrometer (DLS) collaboration in an effort to more firmly establish the mechanism of electron-positron production in 1–5 GeV nucleon-nucleon collisions [1]. The result of bombarding liquid hydrogen and deuterium targets with 4.9 GeV protons yielded a pd/pp ratio for e^+e^- production that was nearly mass independent and ≈ 2. This suggests that either bremsstrahlung is not responsible for the pair production yields or, if it is, that pp is roughly the same as np. However, conventional wisdom said that the dipole of the np system should be much more significant than the quadrupole of the pp system. Many dilepton production calculations have been done on pn, pA and AA systems at these energies using as a starting assumption that np bremsstrahlung dominates over pp [2]–[5]. Even a *complete* Feynman diagram calculation supports this idea [6]. By improving nucleon-nucleon bremsstrahlung calculations we settle this question. We also generalize to some of the inelastic channels: those of one-, two-, and three-pion final states. The cross section to produce pions in nucleon-nucleon scattering at these energies is comparable to or even larger than elastic scattering. One would therefore like to know if a proper treatment of the many-body electrodynamics gives a significant contribution. The pions produced would not only carry away some fraction of the momentum (thereby increasing proton accelerations and therefore radiation) but they would travel very fast since they are relatively massless and if charged, would themselves radiate significantly. These two complementary features could result in rather large contributions to the low-mass dilepton spectrum.

Other possible mechanisms for pair production in these nucleon-nucleon collisions are hadronic decays, two-pion annihilation and perhaps pion-pion bremsstrahlung. Pion-nucleon bremsstrahlung would also contribute but presumably at a lower level. Dalitz decay of π^0 s contribute in a region where experimental acceptance is low, so in this study we neglect them. Contributions from Dalitz decay of the η and radiative decays of the low-lying

nucleon resonances might be important depending upon their production cross sections. We assume two-step processes for the resonances, namely, $NN \to NR \to NN\gamma^*$ (where R might be a Δ or an N^*). Guided by experimental data for the cross sections and analytically continuing the expressions for real photon production to expressions for pairs of soft leptons using relativistic kinematics, we estimate these contributions. Two-pion annihilation was studied by Kapusta and Lichard in an attempt to explain possible structure near $2m_\pi$ in earlier DLS data [7]. What they found was that when acceptance filtered, the results were not peaked near threshold but rather near the ρ mass. The contribution near the peak was consistent with measured dilepton spectra when p_T integrated. Finally, since multiple pion production is likely at these energies, we estimate the contribution from $\pi\pi$ bremsstrahlung in 4.9 GeV pp scattering.

The paper is organized in the following way. In Sec. 2 we present the soft-photon approximation with which we calculate and the particular continuation to finite invariant masses we use. This will include partial corrections to phase space which are absolutely necessary in soft-photon approximations. Then in Sec. 3 we apply the formalism to nucleon-nucleon collisions with very accurate parametrizations for the angular descriptions of elastic scattering. Section 4 contains an application to one-, two-, and three-pion final state many-body bremsstrahlung. The complicated matrix elements are approximated by their resonance structure since these inelastic channels proceed primarily through formation and decay of Δ-isobars. Dalitz decay of the ηs and radiative decays of the low-lying nucleon resonances are estimated in Sec. 5. Inclusion of a model calculation of $\pi^+\pi^-$ annihilation and its contribution to the e^+e^- mass spectrum is shown along with our $\pi\pi$ bremsstrahlung estimates. Also in Sec. 5, we show the sum of the bremsstrahlung, η Dalitz and Δ radiative decays and two-pion annihilation, as compared with dilepton yields in proton-proton collisions from the DLS. Then in Sec. 6, we predict data for true cross sections instead of yields and present theoretical cross sections without any experimental (acceptance) limitations. Finally, in Sec. 7 we summarize our findings concluding that many-body bremsstrahlung is the largest contributor to low-mass dilepton production in nucleon-nucleon collisions at these energies.

2 Soft-Photon Approximation

One very pleasant feature of calculating within a soft-photon approximation is that the complicated algebraic structure of the diagrams separates into two somewhat less complicated pieces. Even if the final state is comprised of $n > 2$ hadrons, the matrix element for soft-photon production simplifies to the purely hadronic counterpart times a multiplicative function describing the complicated electrodynamics of the reaction [8]. Then as long as care is taken to approximately account for neglecting the momentum of the photon in the energy-conserving delta function of phase space, the differential cross section for quasi-elastic scattering while at the same time producing a virtual photon (electron-positron pair) of invariant mass M and energy q_0 is

$$\begin{aligned} \frac{d\sigma^{e^+e^-}}{dM} &= \frac{\alpha^2}{4\pi^4}\frac{1}{Mq_0^2}\widehat{\sigma}(s)\int \delta(q^2-M^2)\delta^4\left(q-(p_+ + p_-)\right)d^4q \\ &\quad \times \frac{d^3p_+ d^3p_-}{E_+E_-}\frac{R_n(s')}{R_n(s)}, \end{aligned} \tag{1}$$

where R_n is n-body phase space [9], $s' = s + M^2 - 2\sqrt{s}q_0$ and

$$\widehat{\sigma}(s) \equiv \int \prod_{i=1}^{n} d^3p_i \left[\frac{d^{3n}\sigma}{\prod_{i=1}^{n} d^3p_i}\right]\left(q_0^2\left|\epsilon\cdot J\right|^2\right). \tag{2}$$

The square-bracketed expression in Eq. (2) is the elastic ($n = 2$) or inelastic ($n > 2$) hadronic cross section and $q_0^2|\epsilon\cdot J|^2$ is the dimensionless electromagnetic *weighting* representing a coherent sum of all radiation fields involved. For this general process $a + b \to 1 + 2 + \ldots + n$, depicted in Fig. 1, the electromagnetic four-current is

$$J^\mu = -\frac{Q_a p_a^\mu}{p_a\cdot q} - \frac{Q_b p_b^\mu}{p_b\cdot q} + \sum_{j=1}^{n}\frac{Q_j p_j^\mu}{p_j\cdot q}, \tag{3}$$

where the Qs are charges in units of the proton charge. In this soft-photon method of calculating it is reasonable to take an angular average over the unobserved internal photon's solid angle. The result of the electromagnetic *weighting* is [10]

$$
\begin{aligned}
q_0^2\,|\epsilon\cdot J|^2 \;=\; & -(Q_a^2+Q_b^2+\sum_{i=1}^{n}Q_i^2) \\
& -2Q_aQ_b(1-\vec{\beta}_a\cdot\vec{\beta}_b)\mathcal{I}(\vec{\beta}_a,\vec{\beta}_b) \\
& +\sum_{i=1}^{n}2Q_aQ_i(1-\vec{\beta}_a\cdot\vec{\beta}_i)\mathcal{I}(\vec{\beta}_a,\vec{\beta}_i) \\
& +\sum_{i=1}^{n}2Q_bQ_i(1-\vec{\beta}_b\cdot\vec{\beta}_i)\mathcal{I}(\vec{\beta}_b,\vec{\beta}_i) \\
& -\sum_{i<j}^{n}2Q_iQ_j(1-\vec{\beta}_i\cdot\vec{\beta}_j)\mathcal{I}(\vec{\beta}_i,\vec{\beta}_j), \qquad (4)
\end{aligned}
$$

where the function

$$
\mathcal{I}(\vec{u},\vec{v}) \;=\; \frac{1}{2\sqrt{\mathcal{R}}}\ln\left|\frac{[\vec{u}\cdot\vec{v}-u^2-\sqrt{\mathcal{R}}\,][\vec{u}\cdot\vec{v}-v^2-\sqrt{\mathcal{R}}\,]}{[\vec{u}\cdot\vec{v}-u^2+\sqrt{\mathcal{R}}\,][\vec{u}\cdot\vec{v}-v^2+\sqrt{\mathcal{R}}\,]}\right|, \qquad (5)
$$

and the scalar

$$
\mathcal{R}=(1-\vec{u}\cdot\vec{v})^2-(1-u^2)(1-v^2). \qquad (6)
$$

The $\vec{\beta}$s are particle velocities $\vec{p}/E$. This function presented in Eqs. (4)–(6) is ultimately responsible for determining the relative strengths of pp and np bremsstrahlung. For $2\to 2$ hadron reactions, this function can be well approximated by a much simpler and much used expression when the momentum transfer is small, e.g. it is proportional to t in np scattering for $t<4m_N^2$ [2]. But we do not make such an assumption because it does not hold generally, a point that we believe is not fully appreciated. We show in Fig. 2 this electromagnetic *weighting* for 4.9 GeV np and pp reactions as a function of center-of-mass scattering angle. As we see, pp is suppressed only at the poles and rises to some rather large value for intermediate angles. For scattering angles in the forward hemisphere pp is larger than np. This is not inconsistent with the assumption that has prevailed in discussions of bremsstrahlung about np dominating pp since the assumption was based on a non-relativistic argument. At 100 MeV kinetic energy, for instance, the maximum value of the pp weighting (at $\cos\theta=0$) is $\approx 4.0\times10^{-3}$, whereas the np weighting at that angle is $\approx 7.0\times10^{-2}$. For brevity, we do not show results at other energies, but already at 1 GeV the np domination breaks down. In the next section we parametrize pp and np angular distributions guided by experimental data, weight them with the functions plotted in Fig. 2 by evaluating Eq. (1), and obtain the e^+e^- invariant mass spectra.

3 Nucleon-Nucleon Bremsstrahlung

The absolute strength of nucleon-nucleon bremsstrahlung depends, among other things, on the differential elastic cross section $d\sigma/dt$. By definition, this is symmetric for pp scattering at any energy, whereas, it is slightly asymmetric for np at energies of interest to this study. This asymmetry can suppress the np bremsstrahlung contribution to dilepton production by a factor 4 for 4.9 GeV reactions as compared with calculations using a symmetric $d\sigma/dt$ [11, 12]. Clearly what is needed in order to minimize uncertainty in normalization are very accurate parametrizations of the experimental data. Functional forms that do quite nicely for energies 1–5 GeV are presented here. First for pp at 4.9 GeV we use

$$\begin{aligned}\frac{d\sigma_{pp}}{d\Omega} &= \exp\{\Theta(\theta-\theta_0)\Theta\left((\pi-\theta_0)-\theta\right)\left(A+B|\theta-\pi/2|^{\gamma}\right) \\ &\quad +\Theta(\theta_0-\theta)(C-D|\theta|^{\delta}) \\ &\quad +\Theta\left(\theta-(\pi-\theta_0)\right)\left(C-D|\pi-\theta|^{\delta}\right)\Big\} \end{aligned} \tag{7}$$

where Θ is the Heavyside-Step function,

$$\begin{aligned} A &= \log\frac{d\sigma_{pp}(\pi/2)}{d\Omega} \\ B &= |\theta_0-\pi/2|^{-\gamma}\log\left(\frac{d\sigma_{pp}(\theta_0)/d\Omega}{d\sigma_{pp}(\pi/2)/d\Omega}\right) \\ C &= \log\frac{d\sigma_{pp}(0)}{d\Omega} \\ D &= |\theta_0|^{-\delta}\log\left(\frac{d\sigma_{pp}(0)/d\Omega}{d\sigma_{pp}(\theta_0)/d\Omega}\right), \end{aligned} \tag{8}$$

and $\gamma = 2.3$, $\delta = 1.6$, $\theta_0 = \pi/6$, $d\sigma_{pp}(0)/d\Omega = 80$ mb/sr, $d\sigma_{pp}(\theta_0)/d\Omega = 0.9$ mb/sr and $d\sigma_{pp}(\pi/2)/d\Omega = 5.0\times10^{-3}$ mb/sr; and then for np scattering again at 4.9 GeV we use

$$\begin{aligned}\frac{d\sigma_{np}}{d\Omega} &= \exp\{\Theta(\theta_0-\theta)\left(A+B|\theta-\theta_0|^{\gamma}\right) \\ &\quad +\Theta\left(\theta-\theta_0\right)\left(C+D|\theta-\theta_0|^{\delta}\right)\Big\}, \end{aligned} \tag{9}$$

$$A = \log\frac{d\sigma_{np}(\theta_0)}{d\Omega}$$

$$
\begin{aligned}
B &= \theta_0^{-\gamma} \log\left(\frac{d\sigma_{np}(0)/d\Omega}{d\sigma_{np}(\theta_0)/d\Omega}\right) \\
C &= \log\frac{d\sigma_{np}(\theta_0)}{d\Omega} \\
D &= |\pi-\theta_0|^{-\delta} \log\left(\frac{d\sigma_{np}(\pi)/d\Omega}{d\sigma_{np}(\theta_0)/d\Omega}\right), \qquad (10)
\end{aligned}
$$

and $\gamma = 2.3$, $\delta = 2.5$, $\theta_0 = 99$ degrees, $d\sigma_{np}(0)/d\Omega = 6.27 \times 10^2$ mb/sr, $d\sigma_{np}(\theta_0)/d\Omega = 1.62 \times 10^{-5}$ mb/sr and $d\sigma_{np}(\pi)/d\Omega = 16.2$ mb/sr.

Comparisons are made with np [13, 14, 15] and pp [16, 17] data in Figs. 3a and 3b. Upon integrating these expressions over the scattering angle, or equivalently over momentum transfers $-(s-4m_N^2) \leq t \leq 0$, we obtain cross sections of 11.9 mb and 11.1 mb for pp and np, respectively. Recall, there is a factor 1/2 in the pp case to avoid double counting of the identical particles.

In order that we might compare to published data on dilepton production, we include the DLS acceptance filter to calculate a yield. The results are then acceptance filtered but not acceptance corrected [1], and they have units of cross section. When Eqs. (7) and (9) are used in Eq. (2), and in turn in Eq. (1) (with acceptance filter and weight included), the resulting spectra differ by a constant factor of ≈ 1.5. That the spectra differ by a constant is a consequence of our soft photon approximation. We show the yields in Fig. 4, where the comparison is absolute. Proton-proton bremsstrahlung is stronger than neutron-proton at this energy! If we construct the ratio of $\sigma(np+pp)/\sigma(pp)$, we find it to be 1.67. Therefore, it is not the measured ratio of order 2 that eliminates bremsstrahlung from being responsible for the e^+e^- yields; one must compare the distributions separately. Upon doing so, one if forced to conclude that simple bremsstrahlung is not responsible for the observed pp yields. One naturally thinks to estimate the inelastic channels' contributions to e^+e^- production. After all, at 5 GeV the cross section is mostly inelastic.

4 Multiple-Hadron Final States

The cross sections to produce up to and including five pions have been measured in 5.5 GeV/c proton-proton collisions [18]. The one, two and perhaps three pion final states are important for our considerations here. Their cross sections are 10.8, 11.4, and 11.7 mb, respectively. At the same time the elastic channel's cross section is 11.3 mb. So clearly, these inelastic channels

cannot be ignored. What is needed are the $NN \to NN\pi$, $NN \to NN\pi\pi$, and $NN \to NN\pi\pi\pi$ matrix elements. One could of course perform a field theory calculation to get a fairly complete description of them. The interactions of π and ρ mesons coupling to a nucleon and a delta are well known. However, the Δ propagator presents some technical difficulty making a full-blown calculation extremely lengthy. Furthermore, even a detailed one-boson-exchange calculation is not guaranteed to produce correct angular behavior for the differential cross section. We pursue a different approach. The process $pp \to np\pi^+$ proceeds primarily through Δ^+ or Δ^{++} excitation of the nucleon, with subsequent decay into a nucleon and the positively charged pion. The corresponding diagrams are shown in Figs. 5a and 5b, with exchange diagrams not explicitly drawn. To this order, there are also effects from Δ^0 excitation as in Fig. 5c. Even though the matrix element for these diagrams contains influences from force-mediating meson-exchange, the resonance structure of the Δ propagator alone accounts reasonably well for what is observed in terms of invariant mass distributions. Therefore, we write the matrix element for the diagrams in Fig. 5 as

$$\begin{aligned} \mathcal{M}_{pp\to np\pi^+} &\propto \frac{1}{\sqrt{2}} \frac{(p_1+p_3)^2 - (m_N+m_\pi)^2}{(p_1+p_3)^2 - m_\Delta^2 + i m_\Delta \Gamma_\Delta} \\ &- \frac{7}{3\sqrt{2}} \frac{(p_2+p_3)^2 - (m_N+m_\pi)^2}{(p_2+p_3)^2 - m_\Delta^2 + i m_\Delta \Gamma_\Delta}, \end{aligned} \tag{11}$$

where $a + b \to 1 + 2 + 3$ corresponds to particles $p + p \to n + p + \pi^+$. With this matrix element, we are neglecting the neutral excitation diagram. We have verified that its inclusion is not significant to the final dilepton spectrum, at least within this approximation. Keeping complexity to an absolute minimum while capturing the essential physics, we choose to neglect contributions from diagrams like the one in Fig. 5c. Then the cross section can be calculated by

$$d\sigma = \frac{2m_N^4}{\sqrt{s(s-4m_N^2)}} \frac{|\mathcal{M}|^2}{(2\pi)^5} \delta^4(p_a + p_b - p_1 - p_2 - p_3) \frac{d^3p_1}{E_1} \frac{d^3p_2}{E_2} \frac{d^3p_3}{2E_3}. \tag{12}$$

This reduces to an integration over the four essential final state variables describing phase space. The normalization of the matrix element is adjusted in order to give a cross section of $\sigma(pp \to np\pi^+) = 8.03$ mb. Similar approximations are done for the matrix elements of the processes $pp \to pp\pi^0$, $np \to nn\pi^+$, $np \to np\pi^0$ and $np \to pp\pi^-$. The cross sections we use are:

2.77 mb for $pp \to pp\pi^0$, 8.03 mb for $np \to nn\pi^+$ and finally, 2.77 mb for both $np \to np\pi^0$ and $np \to pp\pi^-$. Future model calculations are needed to improve on these matrix elements, but for first approximation they are sufficient.

With these hadronic one-pion-production cross sections, we insert into Eq. (2) and subsequently into Eq. (1) in order to calculate each channel's contribution to dilepton production. Three-body phase space can be written as

$$R_3(s) = \int_{(m_N+m_\pi)^2}^{(\sqrt{s}-m_N)^2} ds_2 R_2(s, s_2, m_N^2) R_2(s_2, m_N^2, m_\pi^2). \tag{13}$$

When Eq. (1) is evaluated for the $n = 3$ case under consideration and with the acceptance filter included upon integration over dilepton p_T and rapidity, a yield is obtained that can be directly compared with the simple pp bremsstrahlung presented earlier. In Fig. 6 we show the two single-pion final state contributions superimposed with simple bremsstrahlung. The largest contributor is the channel $pp \to np\pi^+e^+e^-$. For low invariant masses, it is larger than simple bremsstrahlung by nearly an order of magnitude. This many-body contribution has been ignored in previous calculations for dilepton production because it was assumed small. It is clear that such an omission is not justified. The same analysis applied to the np channels gives similar results. Charged nucleon reaction partners are of course important for bremsstrahlung. But we have discovered that since the inelastic cross sections are comparable in size to elastic, having a charged pion in the final state significantly boosts the radiation.

We then proceed to estimate the contributions from the two-pion final states. There are four channels each for pp and np scattering. The same kind of approximations are made in order to arrive at the matrix elements. This time, however, there are two Δ excitations and the isospin factors are different. The general structure of the diagrams is shown in Fig. 7. Again, we are neglecting diagrams that contain delta excitations on the initial lines since they are not essential. The matrix element we use for the process in Fig. 7 is

$$\begin{aligned} \mathcal{M}_{pp\to pp\pi^+\pi^-} \quad &\propto \quad \frac{(p_1+p_3)^2-(m_N+m_\pi)^2}{(p_1+p_3)^2-m_\Delta^2+im_\Delta\Gamma_\Delta}\,\frac{(p_2+p_4)^2-(m_N+m_\pi)^2}{(p_2+p_4)^2-m_\Delta^2+im_\Delta\Gamma_\Delta} \\ &+ \quad \frac{(p_2+p_3)^2-(m_N+m_\pi)^2}{(p_2+p_3)^2-m_\Delta^2+im_\Delta\Gamma_\Delta} \end{aligned}$$

$$\times \frac{(p_1+p_4)^2-(m_N+m_\pi)^2}{(p_1+p_4)^2-m_\Delta^2+im_\Delta\Gamma_\Delta}, \tag{14}$$

where p_1 and p_2 label the protons and $p_3(p_4)$ labels the positive(negative) pion. Similar approximations give the matrix elements for $pp \to pp\pi^0\pi^0$, $pp \to np\pi^+\pi^0$, $pp \to nn\pi^+\pi^+$, and $np \to np\pi^+\pi$, $np \to np\pi^0\pi^0$, $np \to pp\pi^-\pi^0$ and $np \to nn\pi^+\pi^0$. For simplicity, we assume an isospin equivalence forcing a numerical value of 2.85 mb for the cross sections of all two-pion final states. Measured pp channels differ from this by only a small amount, so it is not unreasonable.

The phase space correction this time is $R_4(s')/R_4(s)$, where

$$R_4(s) \;=\; \int_{s_2^-}^{s_2^+}\int_{m_2^-}^{m_2^+} ds_2 dm_2 R_2(s,s_2,m_2)R_2(s_2,m_N^2,m_\pi^2)R_2(m_2,m_N^2,m_\pi^2), \tag{15}$$

with $s_2^- = (m_N+m_\pi)^2$, $s_2^+ = (\sqrt{s}-m_N-m_\pi)^2$, $m_2^- = (m_N+m_\pi)^2$ and $m_2^+ = (\sqrt{s}-\sqrt{s_2})^2$. Naturally, this correction has a tendency to suppress higher massed pairs. The suppression with two pions in the final state is greater than it is having just a single pion. Carrying out the necessary phase space integration we find the resulting contributions to e^+e^- yields from two-pion final states to be intermediate between simple pp bremsstrahlung and the largest single-pion channel. There are enough channels, however, so that when added together the low-mass contribution is slightly larger than that from single-pion final state bremsstrahlung.

Finally, there is the issue of $m > 2$ pion final states. Note that at 4.9 GeV there is enough phase space to allow as many as 12 pions in the final state. The cross section to produce three pions in pp scattering at 5.5 GeV/c is 11.7 mb. By doing a proper treatment of the five-body electrodynamics and by approximating the matrix elements in our by now familiar fashion, we find the contribution important only to the lowest two or three invariant mass bins. Specifically, using a cross section of 2.34 mb for the channel $pp \to np\pi^+\pi^+\pi^-$, we find $dn^{e^+e^-}/dM \approx 8.0\times10^{-5}$ μb/GeV for $M = 0.075$ GeV. Admittedly this seems relatively large; but the five-body phase space correction very strongly suppresses the distribution for increasing invariant mass, bringing it down to 4.0×10^{-6} μb/GeV at $M = 0.500$ GeV. There are five charge configurations for three-pion final states which must all be included. Assuming charge independence for the cross sections, we arrive at our aforementioned value of 2.34 mb for each of these channels. The relative

smallness of the cross sections for four- and five-pion production justifies ignoring them here.

In Figure 8 we show the sum of zero-, one-, two-, and three-pion final-state hadronic bremsstrahlung. One should compare to data only in the low-mass region where this soft-photon approximation is best. Upon doing so, we may conclude that these inelastic channels are responsible for much of the low-mass dilepton yield. A previous dilepton calculation which included a comparison between the soft-photon approximation and a Feynman-diagram method in 4.9 GeV np scattering showed the soft-photon result smaller than the diagram calculation by a factor of 6 at invariant mass 300 MeV. The two results converged to the same curve (as they must) in the limit $M \to 0$ [6]. So one is encouraged that bremsstrahlung might even account for the yields at low-to-intermediate masses.

5 Other sources

Hadronic decays are the next most likely candidate for a mechanism of significant dilepton production. Of the possible hadrons that might be excited or produced in nucleon-nucleon collisions at energies ~ 1 GeV, we find that the η and the Δ contribute the most. The rho and omega are somewhat below the delta, so we ignore them here. The delta has a direct decay channel $\Delta \to N\gamma$ with measured branching ratio 0.6%. The photon might not satisfy the Einstein condition $q^2 = 0$, but instead appear as a virtual (massive) photon. The precise mathematical formulation of the analytical continuation we use is identical to the calculation published first by Gale and Kapusta in Ref. [19].[1] The Δ production cross section we use is the measured value of 5.0 mb. We have also checked the contributions from radiative decay of the first few low-lying N^* s and found them to be small compared to the Δ. Calculation of the eta proceeds in the same way as the estimate from Ref. [1] with one exception. We use the upper limit for the eta production cross section: 0.5 mb. Then a differential cross section is assumed which is gaussian in laboratory rapidity and exponential in transverse mass. For more details see Ref. [1].

At 4.9 GeV, the cross section to produce pions is larger than elastic scattering. The 1, 2, 3, and 4 pion production cross sections in pp scattering are 10.8, 11.4, 11.7 and 1.6 mb, respectively. Since the reaction zone has finite

[1]The acceptance filter we use is Version 1.6, a later release than the one used in Ref. [19].

extent, there is clearly some nonzero probability for pion-pion rescattering. Furthermore, vector dominance would suggest that in such scattering the rho resonance accounts for most of the cross section. It is well known that the rho has an electromagnetic decay channel, so it is reasonable to estimate the contribution to dilepton production through two-pion annihilation. This problem has been solved by Kapusta and Lichard in a search for structure in the dilepton mass spectrum [7]. They found a structure appearing at the rho mass (instead of near $2m_\pi$) when the distribution was acceptance corrected. For details of this kinetic theory calculation see Ref. [7].

Pion-pion rescattering with bremsstrahlung will also contribute to dilepton production. Although the contribution from $\pi\pi \to \pi\pi e^+e^-$ might be rather large [10], we must fold in some probability for two (final-state) pions to scatter, and then sum over all possible scattering energies and charge configurations. This requires complete knowledge of the dynamics. However, an estimate can be obtained from the following relation

$$\left(\frac{d\sigma^{e^+e^-}_{\pi\pi}}{dM}\right)_{\text{rescattering}} = \int_{2m_\pi+M}^{\sqrt{s}-2m_N} dm \;\; \frac{dP}{dm}\left(\frac{d\sigma^{e^+e^-}_{\pi\pi}}{dM}\right)_{\text{brems.}}, \tag{16}$$

where the probability for a pion to rescatter off another (pion) with invariant mass squared $m^2 = (p_{\pi_1} + p_{\pi_2})^2$ in a 4.9 GeV pp collision is

$$\frac{dP}{dm} \approx \left(\frac{d\sigma^{e^+e^-}_{\pi^+\pi^-}}{dm}\right) \Big/ \sigma^{e^+e^-}_{\pi^+\pi^-}. \tag{17}$$

The annihilation cross section $\sigma^{e^+e^-}_{\pi^+\pi^-}$, including a vector dominance form factor, is taken from Eq. (15) of Ref. [2]. Finally, the kinetic theory calculation of Kapusta and Lichard gives an estimate of the differential annihilation cross section [7], $d\sigma^{e^+e^-}_{\pi^+\pi^-}/dm$. Having the probability for rescattering, we take the pion-pion bremsstrahlung expression developed within a soft photon approximation in Ref. [10] and evaluate the (invariant energy) integral in Eq. (16). In practice, this is a finite sum $\sum_i \Delta m_i (dP/dm) \times (d\sigma/dM)_{\text{brems}}$. The resulting contribution to dilepton production is comparable to simple proton-proton bremsstrahlung in the low mass region and intermediate masses while it drops rapidly for pair masses above ≈ 600 MeV. Note that this represents a lower bound on the pion-pion bremsstrahlung contribution for two reasons. Firstly, we have neglected other charge configurations and secondly, the probability calculated with Eq. (17) has experimental acceptance contaminating

the numerator. The contamination reduces the probability in the mass region near threshold and should, in principle, not be there. However, the effect is very small. Since the pion-pion result is comparable to simple proton-proton bremsstrahlung at this energy, it is clearly not dominant. On the other hand, it is not insignificant either and should be considered in future calculations. Without performing a detailed numerical simulation, this is as far as we will take such estimates.

The dilepton spectra arising from (total) bremsstrahlung, hadronic decays and from two-pion annihilation are all presented in Fig. 9. Dalitz decay of the eta peaks at a mass $\approx$ 325 MeV and at a level slightly above bremsstrahlung. Therefore, it is a crucial ingredient in the final spectrum. The delta result is bimodal since, like all our results, it is acceptance filtered. The two peaks appear at 200 MeV and at the rho mass. From this it seems the delta is less important than the eta since the peak at 200 MeV is well below bremsstrahlung, and the other peak is masked behind the contribution from two-pion annihilation.

6 Cross Sections

In the previous sections we have presented dilepton yields since cross sections have not yet been published. Now we include a short section in which we predict the cross section data for 4.9 GeV proton-proton collisions, since they are forthcoming. The dominant processes, mechanisms and calculational methods are exactly the same as we have discussed in the previous sections, with one exception. Here we perform an acceptance correction, and therefore the answer is a true cross section [21]. In Fig. 10 we show the resulting invariant mass distributions of true cross sections for bremsstrahlung, hadronic decays and two-pion annihilation. The prediction is absolute.

Another useful comparison is to present cross sections for the various mechanisms without any experimental limitations included, i.e. without any acceptance effects. This *theoretical* comparison no longer depends on a particular experimental apparatus. In Fig. 11 we show such a comparison. The hadronically inelastic channels contribute significantly in the low-mass region.

7 Summary

We have shown by properly calculating the electromagnetic interference in np and pp scattering and by accurately parametrizing the differential cross sections, that the e^+e^- invariant mass distribution from pp bremsstrahlung is larger than np at 4.9 GeV. The single, double, and triple pion production hadronic cross sections were calculated while approximating the matrix elements by their gross properties of Δ formation and decay. Knowing the cross sections for these inelastic channels in pp scattering, we calculated their contribution to the dilepton mass spectrum. The single-pion production channel (with a charged pion) contributed the most to low-mass pairs. Dalitz decay of the eta contributed roughly at the same level in the narrow window near its peak. Finally, the sum of contributions from simple and inelastic hadronic bremsstrahlung, Dalitz decay of the η, radiative decay of Δ, and from $\pi^+\pi^-$ annihilation, satisfactorily describes the measured pp distribution. We conclude that bremsstrahlung is indeed the largest source of low-mass dileptons in these 4.9 GeV pp collisions, but that it comes from many-body bremsstrahlung.

Although the agreement with experimental data is quite good, it is not perfect. We do not attempt in this paper to achieve a closer fit. Our main goal was to establish the importance of the channels with multi-particle final states in electromagnetic radiation calculations. We have neglected several factors that can be important for precise quantitative interpretation of the experimental data. We have no effects of form factors in our dilepton emission many-body cross sections. In this sense, the curves shown in this work represent a lower bound only. However, we have also neglected interference effects in the radiative resonance decays. These should be carefully examined since they have been shown to be of some importance in both dilepton [6] and photon [22] calculations. Radiative decays from multiple Δ excitations have also been neglected here. Potentially important effects in the pion-nucleon channels have not been treated either. Calculation of these rescattering effects requires complete knowledge of the kinematics which is outside the scope of this paper.

The hadronic inelastic channels will now play a major role in the interpretation and understanding of experimental data at these energies. An immediate consequence of our study is that high energy heavy-ion data will require the use of state-of-the-art many-body numerical simulations, where multiparticle final-state channels and their appropriate electromagnetic weighting

must be included. It is of great importance to study the rise of the contributions with the incident kinetic energy to carefully map out the threshold effects. We eagerly await the upcoming data from the DLS and from HADES, the European dilepton collaboration. While it is true that the proliferation of new channels will complicate the many-body problem, we can on the other hand state that it will no doubt contribute to its richness.

Acknowledgements

We both wish to acknowledge the hospitality of the Theoretical Physics Institute and Physics Department at the University of Minnesota where the initial stage of this work was done. Also, we acknowledge useful discussions with Guy Roche. Our research is supported in part by the Natural Sciences and Engineering Research Council of Canada, a NATO collaborative research grant and the FCAR fund of the Québec government. For this work we also acknowledge the U.S. Department of Energy, grant number DOE/DE-FG02-87ER40328.

References

[1] H. Z. Huang, *et al.* Phys. Lett. **297B**, 233 (1992).

[2] C. Gale and J. Kapusta, Phys. Rev. **C 35**, 2107 (1987);

[3] L. Xiong *et al.*, Phys. Rev. **C 41**, R1355 (1990).

[4] Gy. Wolf *et al.*, Nucl. Phys. **A517**, 615 (1990).

[5] K. Haglin, C. Gale and J. Kapusta, Phys. Lett. **224B**, 433 (1989).

[6] K. L. Haglin, Annals of Physics, **212**, 84 (1991).

[7] J. Kapusta and P. Lichard, Phys. Rev. **C 40**, R1574 (1989).

[8] L. Heller, in *Soft Lepton Pair and Photon Production*, edited by J. A. Thompson (Nova Science, 1992), p. 1.

[9] E. Byckling and K. Kajantie, *Particle Kinematics* (John Wiley & Sons, 1973).

[10] K. Haglin, C. Gale and V. Emely'anov, Phys. Rev. **D 46**, 4802 (1992); Phys. Rev. **D 47**, 973 (1993).

[11] L. A. Winckelmann *et al.*, Phys. Lett. **298B**, 22 (1993).

[12] K. Haglin and C. Gale, in *Advances in Nuclear Dynamics*, Proceedings of the 9th Winter Workshop on Nuclear Dynamics, edited by W. Bauer and B. Back (World Scientific, to be published).

[13] J. L. Stone, *et al.*, Phys. Rev. Lett. **38**, 1315 (1977); Phys. Rev. Lett. **38**, 1317 (1977).

[14] E. L. Miller *et al.*, Phys. Rev. Lett. **16**, 984 (1971).

[15] M. L. Perl *et al.*, Phys. Rev. **D 1**, 1857 (1970).

[16] I. Ambats, *et al.*, Phys. Rev. **D 9**, 1179 (1974).

[17] R. C. Kammerud *et al.*, Phys. Rev. **D 4**, 1309 (1971).

[18] G. Alexander *et al.*, Phys. Rev. **154**, 1284 (1967).

[19] C. Gale and J. Kapusta, Phys. Rev. **C 40**, 2397 (1989).

[20] K. Jaeger *et al.*, Phys. Rev. **D 11**, 1756 (1975).

[21] The DLS acceptance filter determines detectable phase space for the lepton pair as well as a weighting $1/w$ for each region in this space. Yields are calculated with the weighting multiplying $d\sigma/dyd^2p_T$ upon integration over dilepton phase space, while cross sections are calculated without.

[22] C. Song, University of Minnesota preprint NUC–MINN–93/2-T; to be published in Phys. Rev. **C**.

Figure captions

1. Hadron-hadron collision with an n-particle final state where the arrows indicate momentum flow. A coherent sum of radiation for all charged external lines is computed.

2. Dimensionless electromagnetic *weighting* as it depends on the center-of-mass scattering angle in 4.9 Gev nucleon-nucleon collisions.

3. Parametrizations of np and pp differential cross sections in (a) and (b), respectively. Experimental data are from (a) Refs. [16, 17], and (b) Refs. [13, 14, 15].

4. Dilepton yield from simple pp and np bremsstrahlung as compared with DLS data from Ref. [1] for 4.9 GeV proton-proton (open circles) and proton-deuteron (solid squares) inclusive reactions. Our pp result is shown as the dashed histogram, np is shown as the dotted histogram, and an approximate $pd = pp + np$ is shown as the solid histogram.

5. Pion production diagrams proceed through Δ^+ formation and decay as in (a), through Δ^{++} formation and decay as in (b) and through Δ^0 excitation as in (c). The exchanged meson ϕ might be a pion, a rho-meson, or some other boson.

6. Dilepton yields obtained from $NN \to NN\pi$ bremsstrahlung as compared with simple nucleon-nucleon bremsstrahlung, and with pp data.

7. Two-pion-production diagrams proceed via $NN \to \Delta\Delta \to NN\pi\pi$.

8. The sum of bremsstrahlung contributions from NN, $NN\pi$, $NN\pi\pi$, and $NN\pi\pi\pi$ final states in pp scattering. Data are again pp results from the Bevalac.

9. Dilepton yields from various mechanisms: bremsstrahlung is presented as solid squares, radiative decay of the Δ is presented as solid triangles, Dalitz decay of the η is shown as open squares, two-pion annihilation is shown as open diamonds, and finally, the sum of all contributions shown as the solid histogram.

10. Cross section (invariant mass distributions) from various mechanisms: bremsstrahlung is presented as solid squares, radiative decay of the Δ is presented as solid triangles, Dalitz decay of the η is shown as open squares, two-pion annihilation is shown as open diamonds and finally, the sum of all contributions shown as the solid histogram.

11. Cross sections without any experimental acceptance included. Labels indicate the following mechanisms: (a) simple proton-proton bremsstrahlung in the solid line, (b)–(e) are $pp\pi^0$ in the dotted line, $np\pi^+$ in the short-dashed line, $pp\pi^+\pi^-$ in the dot-dashed line and $np\pi^+\pi+\pi^-$ final-state bremsstrahlung in the long-dashed line; (f) is eta Dalitz decay and finally, radiative Delta decay is shown in curve (g).

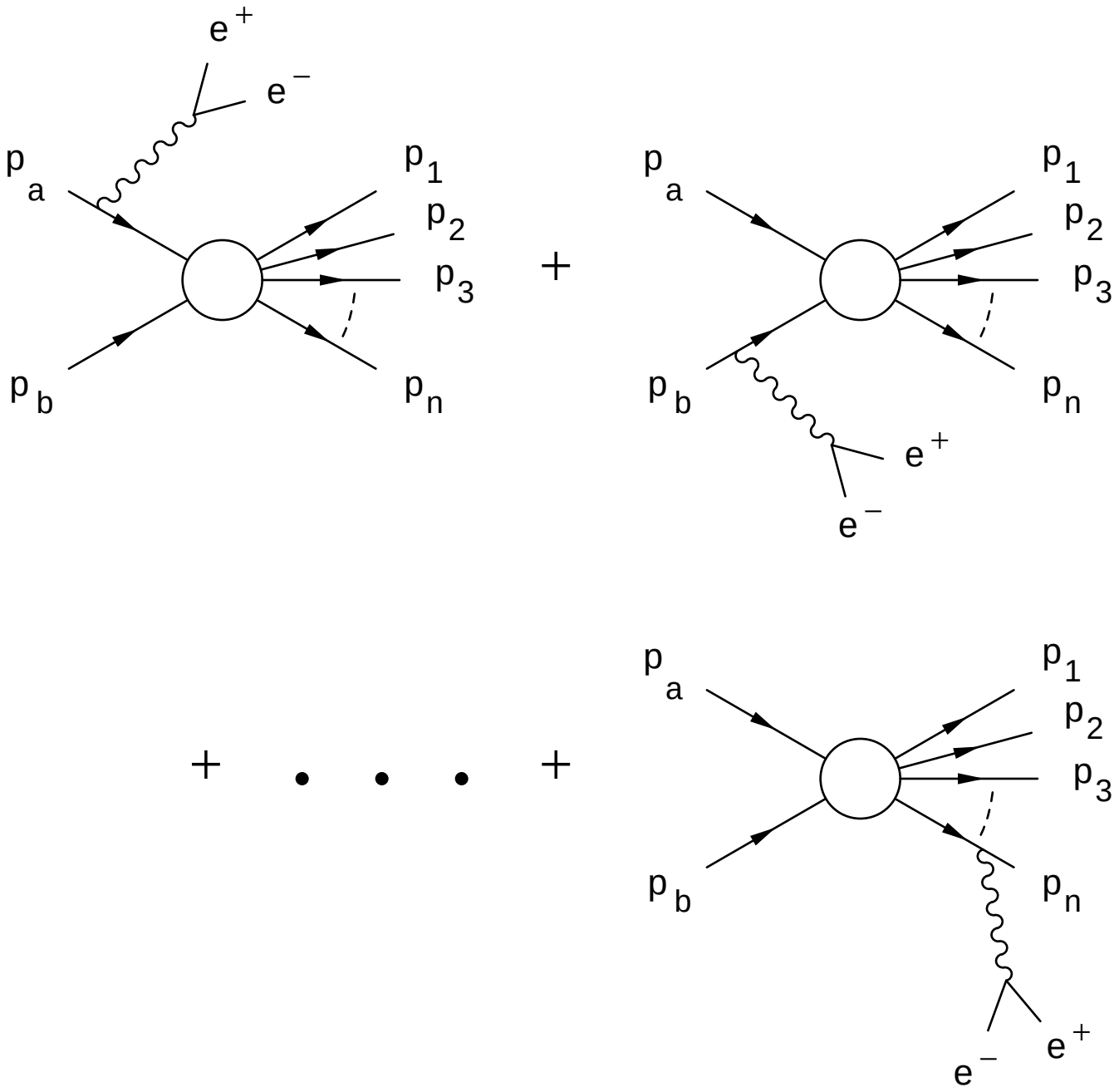

Figure 1

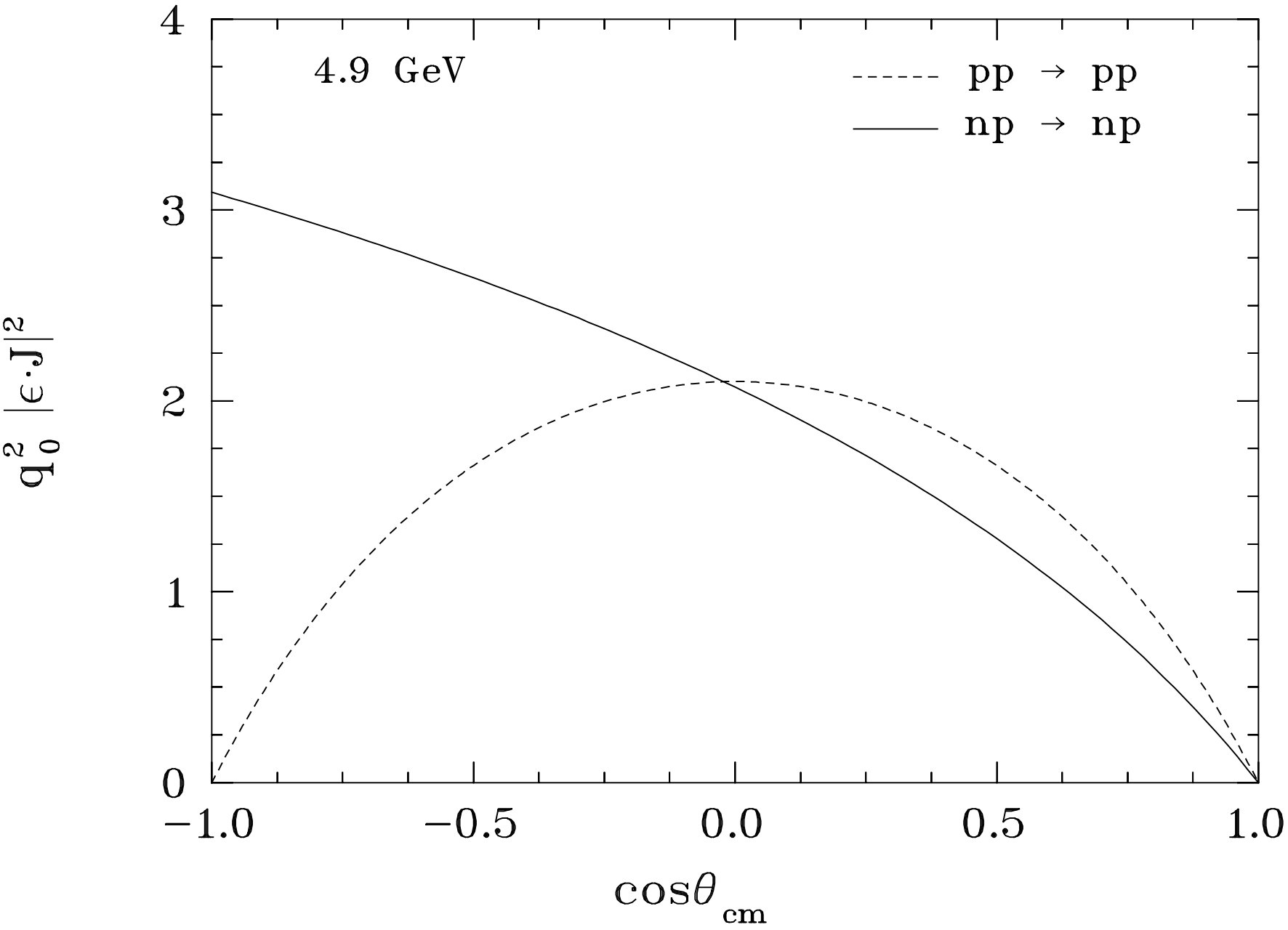
4.9 GeV
pp → pp
np → np
$q_0^2\ |\epsilon \cdot J|^2$
$\cos\theta_{cm}$
0
1
2
3
4
−1.0
−0.5
0.0
0.5
1.0

Figure 2

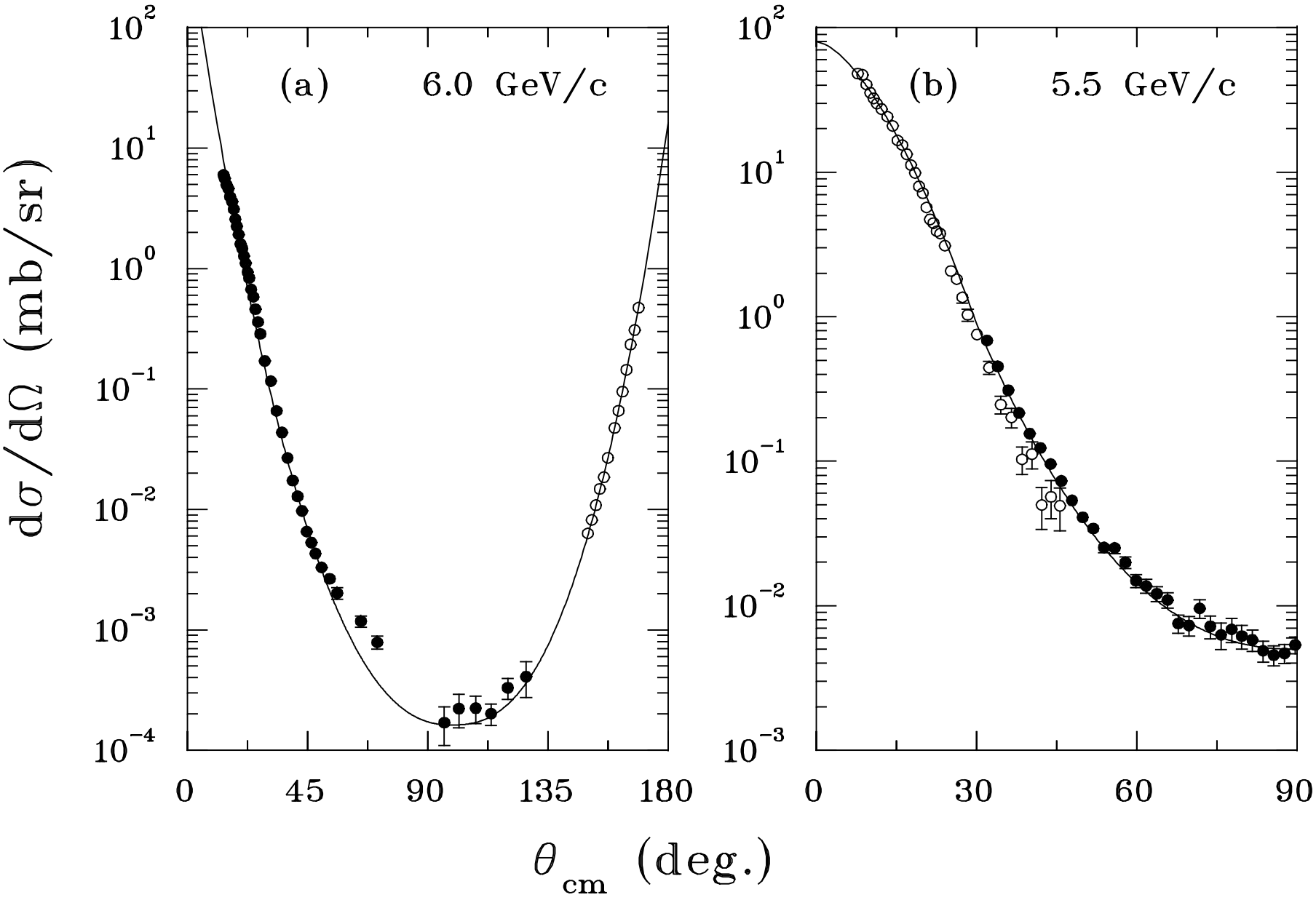
(a) 6.0 GeV/c
(b) 5.5 GeV/c
dσ/dΩ (mb/sr)
θ cm (deg.)
10^2
10^1
10^0
10^-1
10^-2
10^-3
10^-4
0
45
90
135
180
30
60

Figure 3

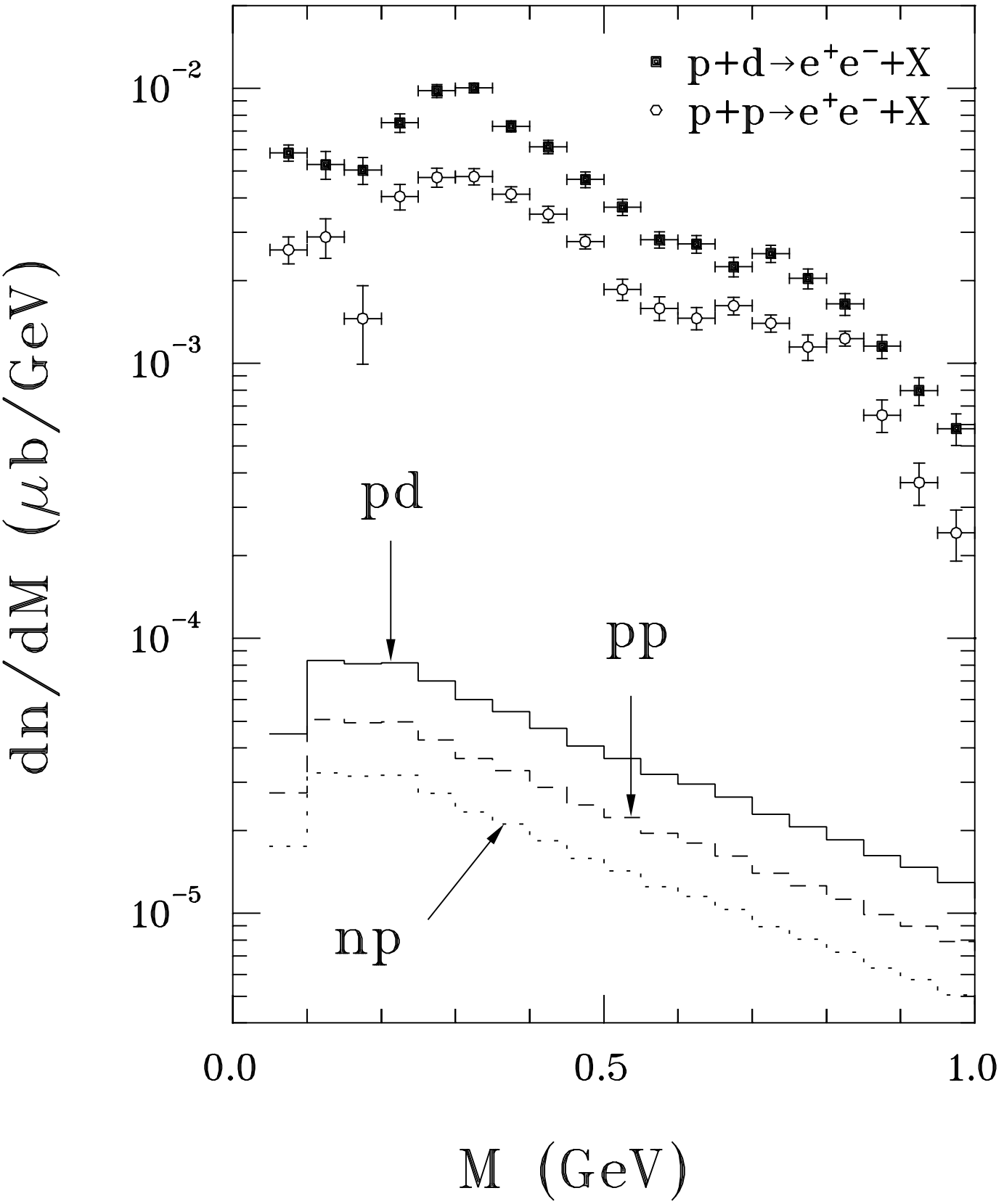

Figure 4

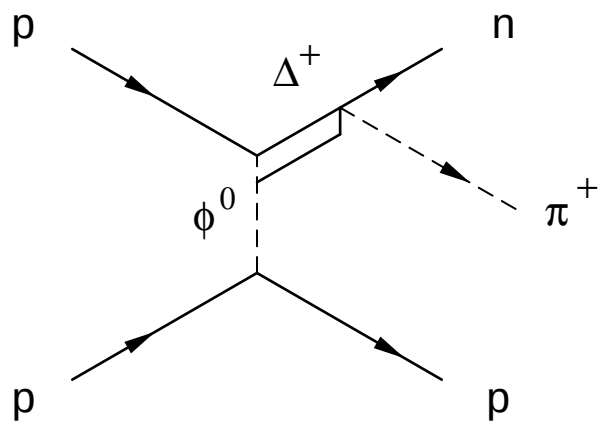

(a)

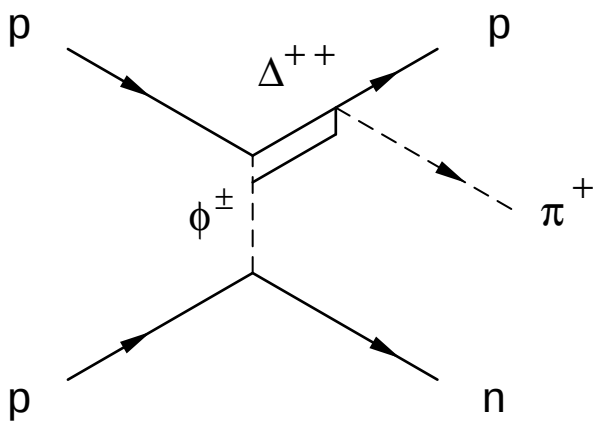

(b)

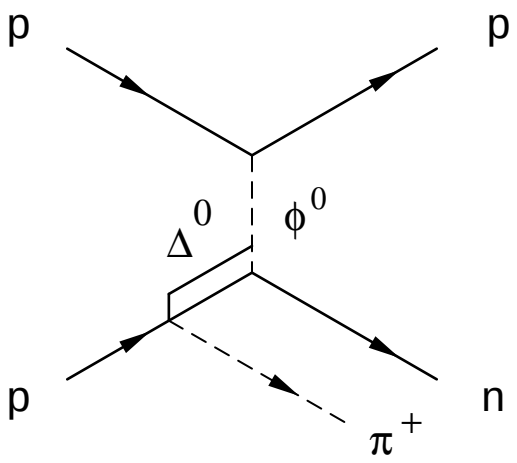

(c)

Figure 5

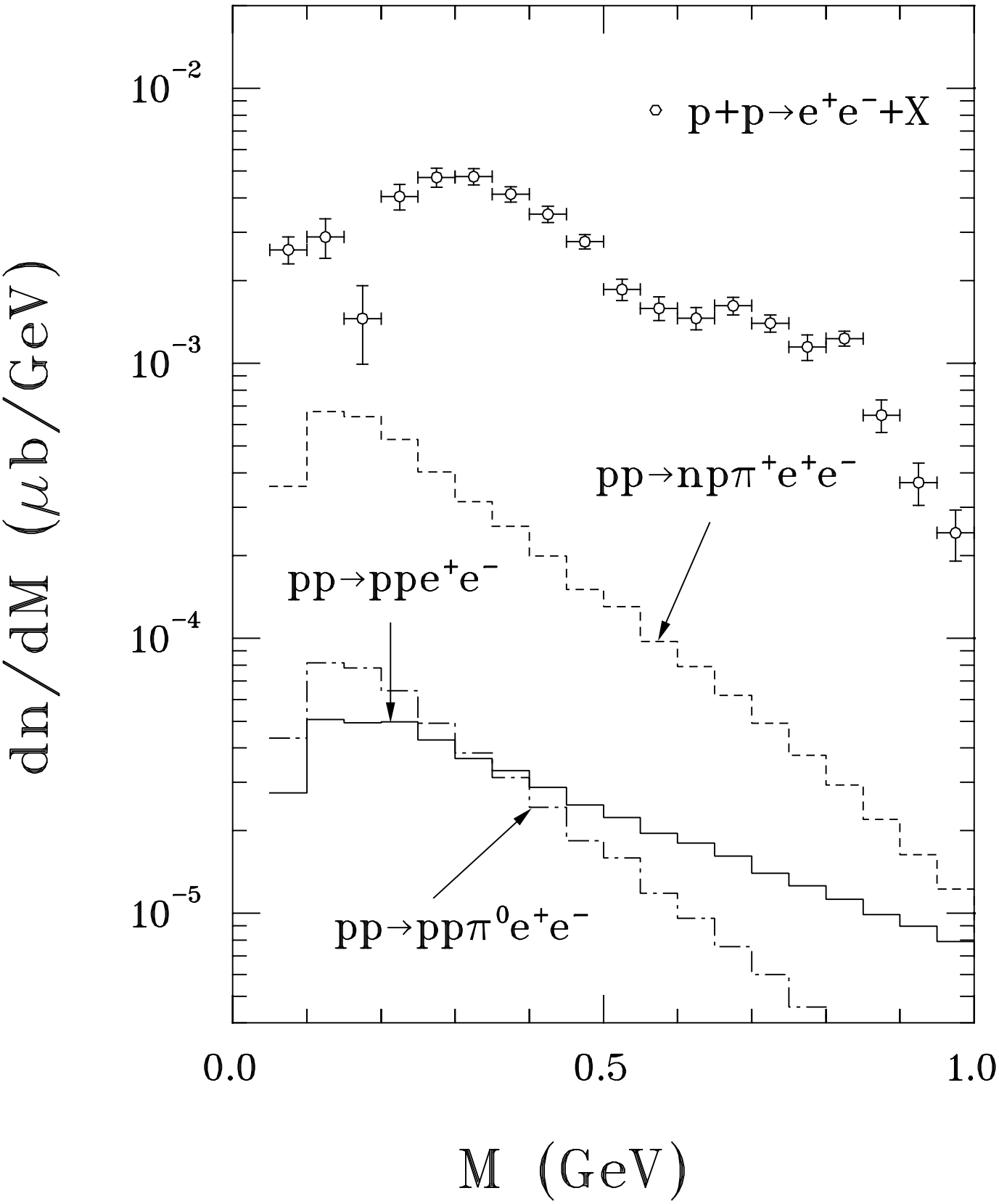
10^{-2}
10^{-3}
10^{-4}
10^{-5}
dn/dM (μb/GeV)
p+p→e⁺e⁻+X
pp→npπ⁺e⁺e⁻
pp→ppe⁺e⁻
pp→ppπ⁰e⁺e⁻
0.0
0.5
1.0
M (GeV)

Figure 6

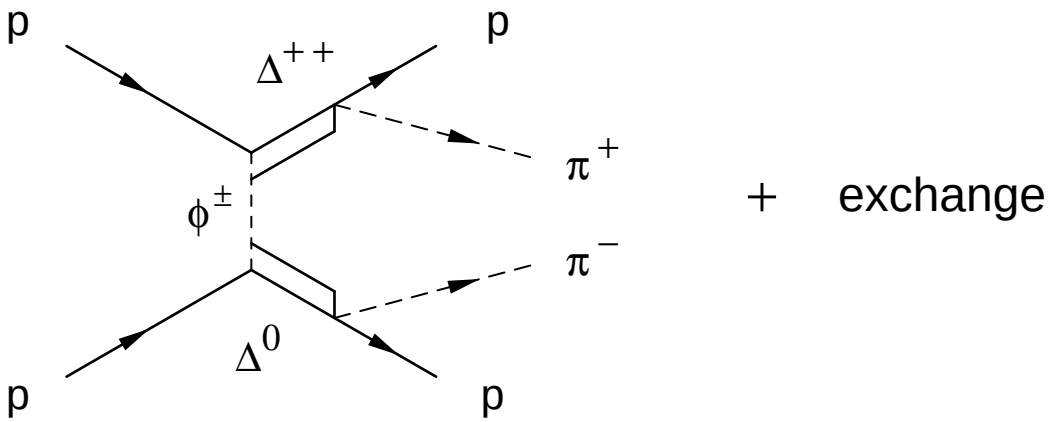

Figure 7

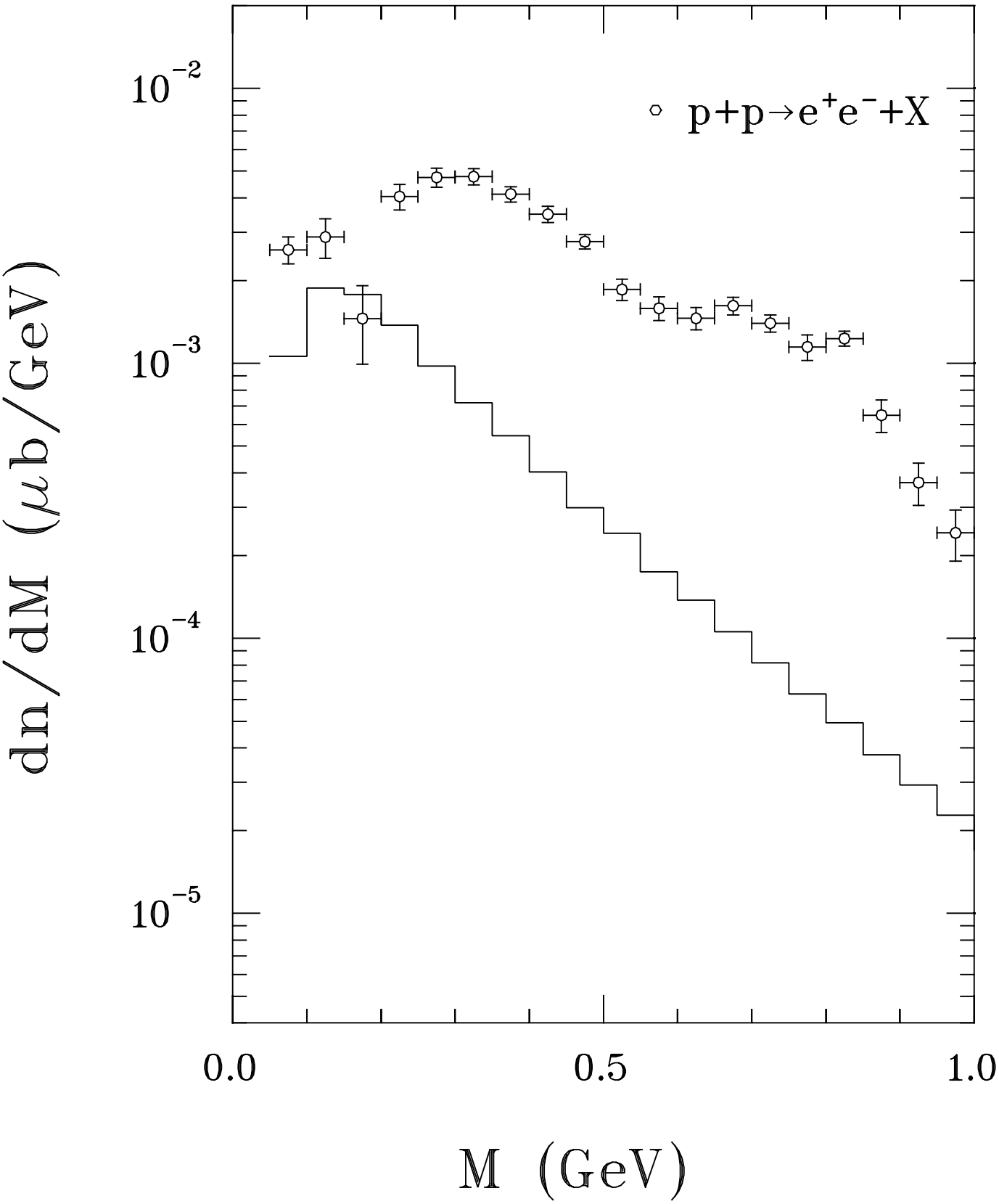

Figure 8

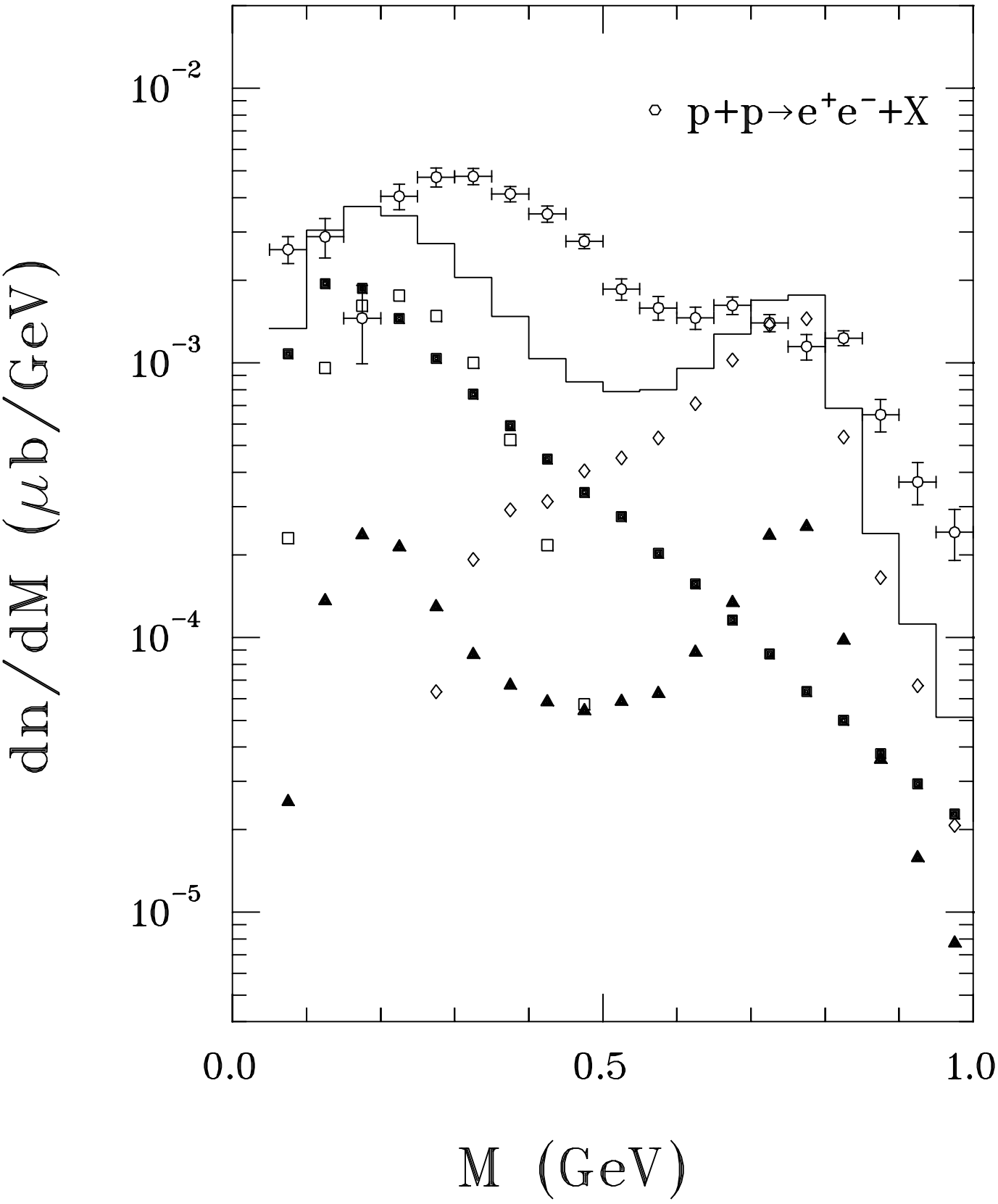

Figure 9

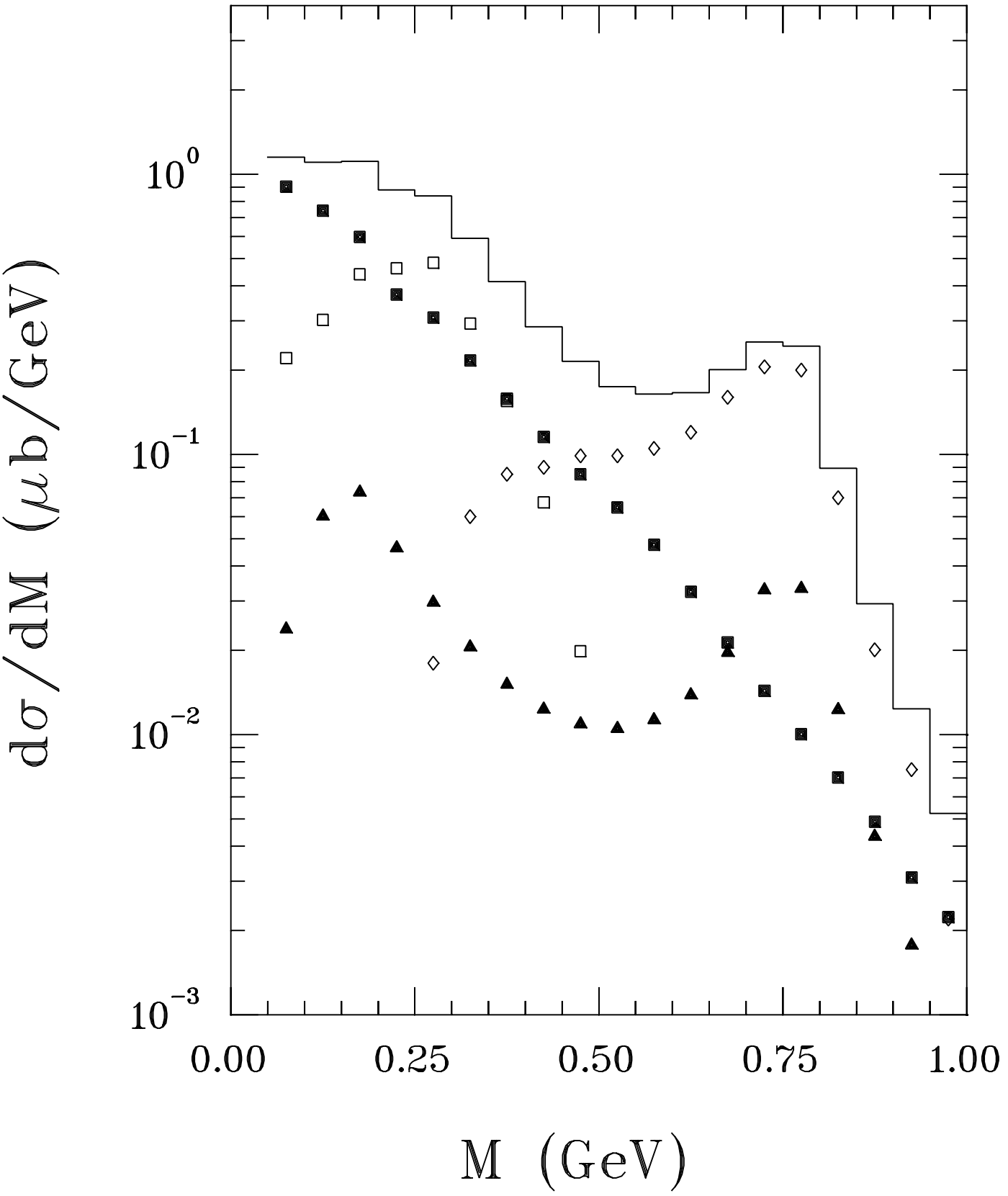

Figure 10

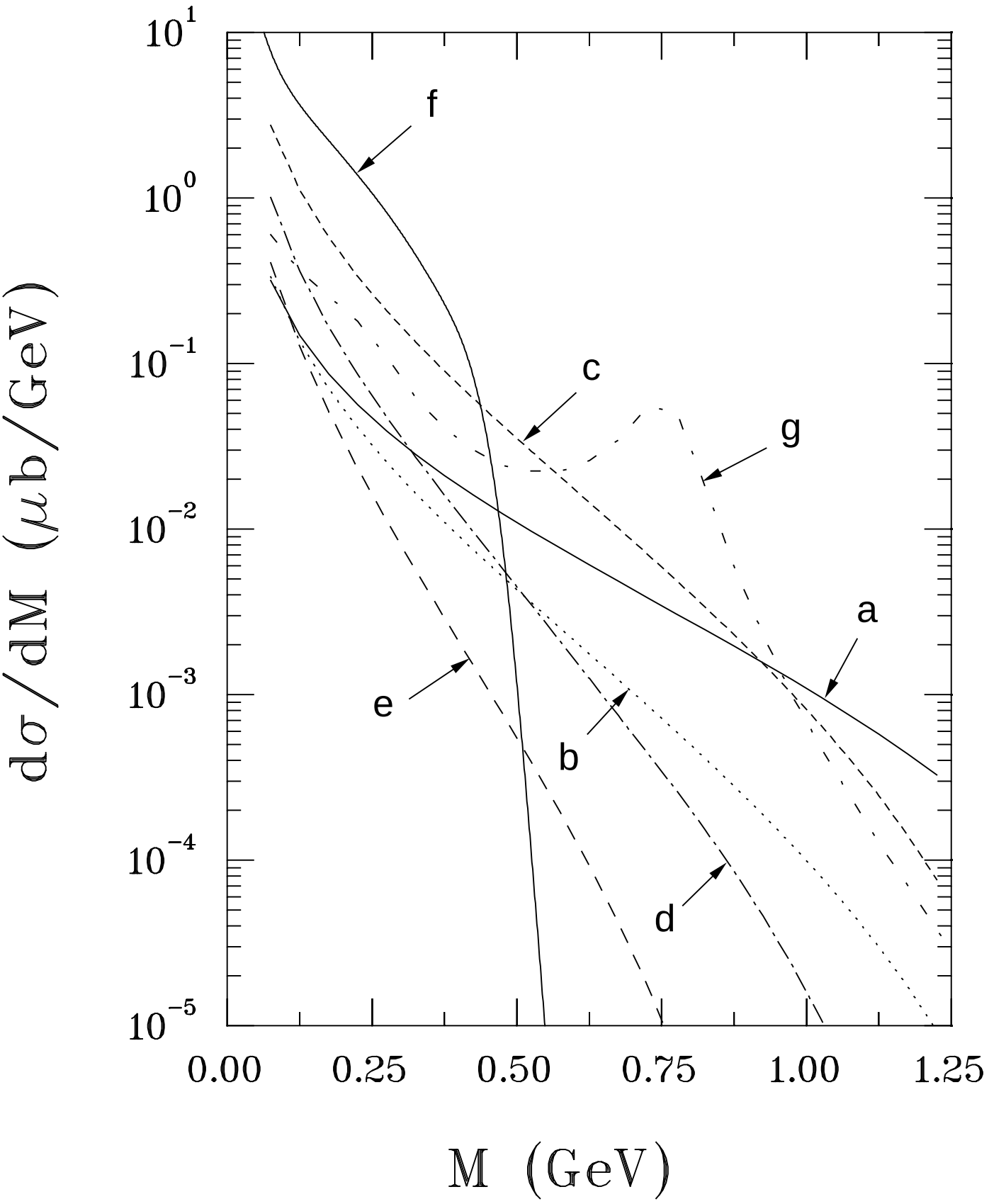
10^1
10^0
10^{-1}
10^{-2}
10^{-3}
10^{-4}
10^{-5}
$d\sigma/dM\ (\mu b/GeV)$
0.00
0.25
0.50
0.75
1.00
1.25
M (GeV)
f
c
g
a
e
b
d

Figure 11